Modeling and Optimization of Active Power Filter Based on a Switched Linear System

Hui Song, Eun-Sung Gil, Kwan-Ho Chun, and Sang-Ho Park

***Abstract*—In this paper, modeling of a three-phase Active Power Filter (APF) considering hybrid dynamics is investigated. A shunt active filter is considered to compensate for the current disturbances from the utility load. Power electronic circuits using APFs are considered as hybrid systems, and the concepts and theories of switched linear systems are introduced to model converter control systems. First, a three-phase converter system is equivalent to a switch linear system (ESLS) based on space vector pulse-width modulator (SVPWM) theory. Then, an ESLS is further transformed into a linear equivalent switch linear system by linearization. Finally, an energy-to-energy (EE) controller is designed.**

***Index Terms*—Active power filter, switched linear system, pulse width modulated.**

I. Introduction

In recent years, various power semiconductor devices such as power diodes, thyristors, power transistors, P-MOSFETs, and IGBTs have been introduced and steadily developed. Power switching devices are being widely used in various power electronic circuits. During the operation of a power switch, power electronic circuits will show different topologies. Conventional power electronic circuit modeling uses the state-space averaging method, the average value of the equivalent circuit, the phase plane method, a large signal equivalent circuit model of unity, and so on. These modeling methods approximate their results to some extent and do not calculate exact amounts for the described system. In addition, we know that system modeling is an important tool and a prerequisite for researching systems. A good model can be helpful in system analysis. Thus, the question is how to accurately describe various kinds of circuit topologies that occur during the operation of a power switch, using a model.

With the development of modern control theory, the theory of hybrid switching systems for power electronic circuit analysis and design provides a new way of thinking. A hybrid system is defined as consisting of a discrete event dynamic system (DEDS) and a continuous variable dynamic system (CVDS). [1] Obviously, power electronic circuits owing to their own switching characteristics comprise a typical amount of hybrid systems. As an important type of hybrid system, a switching system can more accurately describe the essential characteristics of power electronic circuits.

A hybrid switching system model description for power electronic circuits has the following characteristics: First, the model is completely accurate. There are no approximations. Various topologies of a converter can be reflected in the actual work, which reflects the essential characteristics of a hybrid switching system. Second, the model has very good uniformity. If various topologies of a converter are established, the first part of the model can be determined. Third, the basic characteristics of the control system can be easily analyzed. These characteristics include controllability, observability, and stability. Fourth, we are no longer limited to linear theoretical analysis and can model directly from the hybrid system. Proposing new control strategies and better system optimization will be possible [2].

II. Linear System Model of APF

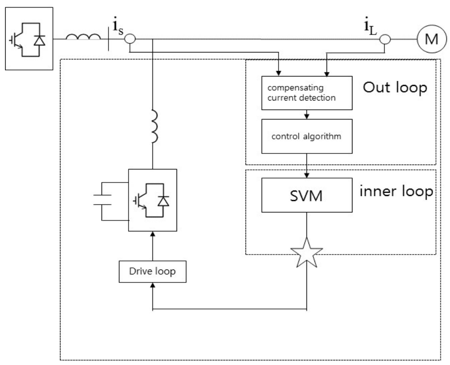

Fig. 1. The structure of APF.

The APF [3]-[5] circuit is a typical example of power electronics. Its structure is shown in Fig. 1. As seen in the figure, the desired APF compensation current is determined through the detection system and the load current calculation, and then through a specific control algorithm to calculate the original closing of each switch-off time by the drive circuit to achieve the original control. Fig. 2 is a three-phase active filter circuit that is parallel with the load [6]. Its advantages are simple structure, small size, and high efficiency. The detection system detects the reference signal i^*. In controlling six switches by turning them off and on, the APF generates a current i track i^* in order to achieve compensation. $L_a = L_b = L_c = L$ are three-phase filter inductors, $r_{ca} = r_{cb} = r_{cc} = r$ are the equivalent resistances of the inductors, C_{dc} is the DC capacitor, V_{sj} is the system supply voltage, V_{cj} is the APF output voltage, r_{lj} is the

Manuscript received September 15, 2016; revised February 15, 2017. This research was supported by Korea Electric Power Corporation through the Korea Electrical Engineering & Science Research Institute (grant number R15XA03-09 15534).

Hui Song, Eun-Sung Gil and Kwan-Ho Chun are with Chungnam National University, South Korea (e-mail: khchun@cnu.ac.kr).

Sang-Ho Park is with Power system lab at the KEPCO Research Institute, South Korea.

doi: 10.18178/jocet.2017.5.6.413

equivalent load resistance, r_{sj} is the resistance to the system power supply, and V_{dc} is the DC capacitor voltage.

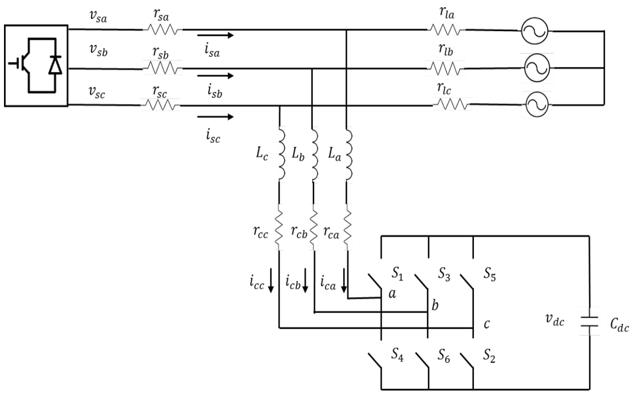

Fig. 2. A three-phase active filter.

If the system load is disturbed, the system model can be expressed as follows:

$$\begin{cases} v_{sa} = L\dfrac{di_{ca}}{dt} + r_{ca}i_{ca} + r_{sa}(i_{ca} + i_{la} + \omega_{la}) + V_{an} + V_{nN} \\ v_{sb} = L\dfrac{di_{cb}}{dt} + r_{cb}i_{cb} + r_{sb}(i_{cb} + i_{lb} + \omega_{lb}) + V_{bn} + V_{nN} \\ v_{sc} = L\dfrac{di_{cc}}{dt} + r_{cc}i_{cc} + r_{sc}(i_{cc} + i_{lc} + \omega_{lc}) + V_{cn} + V_{nN} \end{cases} \quad (1)$$

where ω represents a three-phase interference signal. Represented by the switch status s, its value is as follows:

$$S_a = \begin{cases} 1 & \mathrm{S_1\ close\ and\ S_4\ open} \\ 0 & \mathrm{S_4\ close\ and\ S_1\ open} \end{cases}$$
$$S_b = \begin{cases} 1 & \mathrm{S_3\ close\ and\ S_6\ open} \\ 0 & \mathrm{S_6\ close\ and\ S_3\ open} \end{cases}$$
$$S_c = \begin{cases} 1 & \mathrm{S_5\ close\ and\ S_2\ open} \\ 0 & \mathrm{S_2\ close\ and\ S_5\ open} \end{cases}$$

Then, the following holds:

$$\begin{cases} V_{an} = S_a \cdot V_{dc} \\ V_{bn} = S_b \cdot V_{dc} \\ V_{cn} = S_c \cdot V_{dc} \end{cases} \quad (2)$$

$$V_{aN} + V_{bN} + V_{cN} = 0 \quad (3)$$

The formula can be obtained by inserting (2) and (3) into equation (1):

$$\frac{di_{cj}}{dt} = -\frac{r + r_{sj}}{L} i_{cj} - \frac{r_{sj}}{L}(i_{lj} + \omega_{lj}) - \frac{1}{L}(S_j - \frac{1}{3}\sum_{m=a,b,c} S_m) V_{dc} + \frac{v_{sj}}{L}$$

Thus, the switching function is

$$S_{jN} = S_j - \frac{1}{3}\sum_{m=a,b,c} S_m \quad , \quad j = a,b,c$$

This can be verified in the following manner

$$C_{dc}\frac{dV_{dc}}{dt} = \sum_{m=a,b,c} S_m i_{cm} = \sum_{m=a,b,c} S_{mN} i_{cm}$$

System (1) after the simplified equation of state can be reduced as follows:

$$\begin{bmatrix} \dfrac{di_{ca}}{dt} \\ \dfrac{di_{cb}}{dt} \\ \dfrac{dV_{dc}}{dt} \end{bmatrix} = \begin{bmatrix} -\dfrac{r + r_{sa}}{L} & 0 & -\dfrac{S_{aN}}{L} \\ 0 & -\dfrac{r + r_{sb}}{L} & -\dfrac{S_{bN}}{L} \\ \dfrac{2S_{aN} + S_{bN}}{C_{dc}} & \dfrac{S_{aN} + 2S_{bN}}{C_{dc}} & 0 \end{bmatrix} \begin{bmatrix} i_{ca} \\ i_{cb} \\ V_{dc} \end{bmatrix} + \begin{bmatrix} \dfrac{v_{sa}}{L} - \dfrac{r_{sa}}{L} i_{la} \\ \dfrac{v_{sb}}{L} - \dfrac{r_{sb}}{L} i_{lb} \\ 0 \end{bmatrix} + \begin{bmatrix} -\dfrac{r_{sa}}{L} \\ -\dfrac{r_{sb}}{L} \\ 0 \end{bmatrix}^T \begin{bmatrix} \omega_{la} \\ \omega_{lb} \\ 0 \end{bmatrix} \quad (4)$$
$$= \mathbf{A}(S_{aN}, S_{bN})\mathbf{x} + \mathbf{b}_2 + \mathbf{b}_1\boldsymbol{\omega}$$

This result is a three-phase APF switching dynamic model. To achieve load current compensation, select the output function:

$$y = \mathbf{C}[i_{ca} \quad i_{cb} \quad V_{dc}]^T$$

where $\mathbf{x}$, $\boldsymbol{\omega}$, $(S_{aN}, \ S_{bN})$, and y are the state vector of the APF, the interference vector, and the input and output, respectively. $(S_{aN}, \ S_{bN})$, $\mathbf{b}_1$, $\mathbf{b}_2$, and $\mathbf{C}$ are coefficients for the operating mode.

III. Equivalent Switch Linear Systems of APF

This paper will use the SV-PWM [6], [7] method. Fig. 3 shows the reference signal in the first sector.

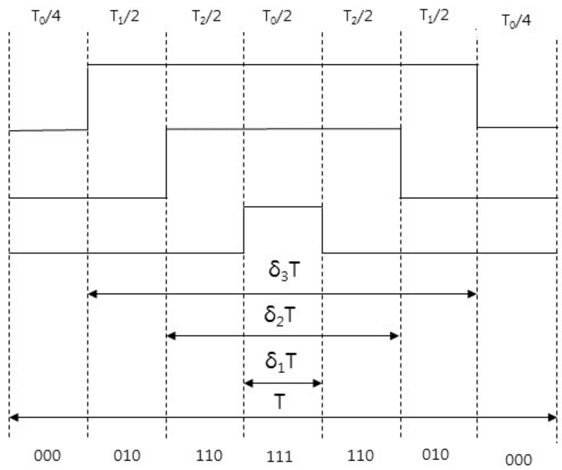

Fig. 3. Seven subintervals of time.

One PWM cycle has seven subintervals of time, within each subinterval corresponding to a different state. To simplify the calculation, Fig. 3 is rearranged to give Fig. 4. Then, in one period, the SVPWM generates four subintervals of time. To determine the PWM waveform, we just need to calculate d_1, d_2 and d_3.

Suppose the reference signal is at the first sector. System (4) can be seen as a switched linear system consisting of four linear subsystems. [See formula (5).] The values of the switching function of each subsystem are shown in Table I.

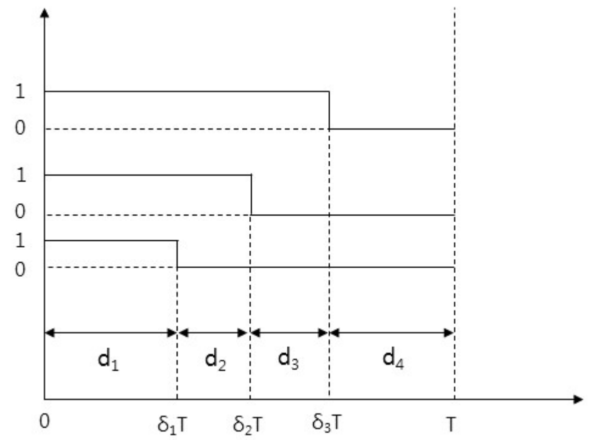

Fig. 4. Four subintervals of time.

TABLE I: THE VALUES OF THE SWITCHING FUNCTION OF EACH SUBSYSTEM

S	sys1 (111)	sys2 (010)	sys1 (011)	sys4 (000)
S_{aN}	0	1/3	2/3	0
S_{bN}	0	1/3	-1/3	0

$$\begin{bmatrix} \frac{di_{ca}}{dt} \\ \frac{di_{cb}}{dt} \\ \frac{dV_{dc}}{dt} \end{bmatrix} = \begin{bmatrix} -\frac{r+r_{sa}}{L} & 0 & 0 \\ 0 & -\frac{r+r_{sb}}{L} & 0 \\ 0 & 0 & 0 \end{bmatrix} \begin{bmatrix} i_{ca} \\ i_{cb} \\ V_{dc} \end{bmatrix} + \begin{bmatrix} \frac{v_{sa}}{L} - \frac{r_{sa}}{L} i_{la} \\ \frac{v_{sb}}{L} - \frac{r_{sb}}{L} i_{lb} \\ 0 \end{bmatrix} + \begin{bmatrix} -\frac{r_{sa}}{L} \\ -\frac{r_{sb}}{L} \\ 0 \end{bmatrix}^T \begin{bmatrix} \omega_{la} \\ \omega_{lb} \\ 0 \end{bmatrix} \tag{5a}$$
$$= \mathbf{A}_1 \mathbf{x} + \mathbf{b}_2 + \mathbf{b}_1 \boldsymbol{\omega}$$

$$\begin{bmatrix} \frac{di_{ca}}{dt} \\ \frac{di_{cb}}{dt} \\ \frac{dV_{dc}}{dt} \end{bmatrix} = \begin{bmatrix} -\frac{r+r_{sa}}{L} & 0 & -\frac{1}{3L} \\ 0 & -\frac{r+r_{sb}}{L} & -\frac{1}{3L} \\ \frac{1}{C_{dc}} & \frac{1}{C_{dc}} & 0 \end{bmatrix} \begin{bmatrix} i_{ca} \\ i_{cb} \\ V_{dc} \end{bmatrix} + \begin{bmatrix} \frac{v_{sa}}{L} - \frac{r_{sa}}{L} i_{la} \\ \frac{v_{sb}}{L} - \frac{r_{sb}}{L} i_{lb} \\ 0 \end{bmatrix} + \begin{bmatrix} -\frac{r_{sa}}{L} \\ -\frac{r_{sb}}{L} \\ 0 \end{bmatrix}^T \begin{bmatrix} \omega_{la} \\ \omega_{lb} \\ 0 \end{bmatrix} \tag{5b}$$
$$= \mathbf{A}_2 \mathbf{x} + \mathbf{b}_2 + \mathbf{b}_1 \boldsymbol{\omega}$$

$$\begin{bmatrix} \frac{di_{ca}}{dt} \\ \frac{di_{cb}}{dt} \\ \frac{dV_{dc}}{dt} \end{bmatrix} = \begin{bmatrix} -\frac{r+r_{sa}}{L} & 0 & -\frac{2}{3L} \\ 0 & -\frac{r+r_{sb}}{L} & \frac{1}{3L} \\ \frac{1}{C_{dc}} & 0 & 0 \end{bmatrix} \begin{bmatrix} i_{ca} \\ i_{cb} \\ V_{dc} \end{bmatrix} + \begin{bmatrix} \frac{v_{sa}}{L} - \frac{r_{sa}}{L} i_{la} \\ \frac{v_{sb}}{L} - \frac{r_{sb}}{L} i_{lb} \\ 0 \end{bmatrix} + \begin{bmatrix} -\frac{r_{sa}}{L} \\ -\frac{r_{sb}}{L} \\ 0 \end{bmatrix}^T \begin{bmatrix} \omega_{la} \\ \omega_{lb} \\ 0 \end{bmatrix} \tag{5c}$$
$$= \mathbf{A}_3 \mathbf{x} + \mathbf{b}_2 + \mathbf{b}_1 \boldsymbol{\omega}$$

$$\begin{bmatrix} \frac{di_{ca}}{dt} \\ \frac{di_{cb}}{dt} \\ \frac{dV_{dc}}{dt} \end{bmatrix} = \begin{bmatrix} -\frac{r+r_{sa}}{L} & 0 & 0 \\ 0 & -\frac{r+r_{sb}}{L} & 0 \\ 0 & 0 & 0 \end{bmatrix} \begin{bmatrix} i_{ca} \\ i_{cb} \\ V_{dc} \end{bmatrix} + \begin{bmatrix} \frac{v_{sa}}{L} - \frac{r_{sa}}{L} i_{la} \\ \frac{v_{sb}}{L} - \frac{r_{sb}}{L} i_{lb} \\ 0 \end{bmatrix} + \begin{bmatrix} -\frac{r_{sa}}{L} \\ -\frac{r_{sb}}{L} \\ 0 \end{bmatrix}^T \begin{bmatrix} \omega_{la} \\ \omega_{lb} \\ 0 \end{bmatrix} \tag{5d}$$
$$= \mathbf{A}_4 \mathbf{x} + \mathbf{b}_2 + \mathbf{b}_1 \boldsymbol{\omega}$$

Formula (5) shows each subsystem of an APF as a continuous variable dynamic system. The switching operation of each subsystem is a discrete event dynamic system. State changes from x0 to x through the intermediate state $\mathbf{x}_0 \xrightarrow{1} \mathbf{x}^{\delta_1} \xrightarrow{2} \mathbf{x}^{\delta_2} \xrightarrow{3} \mathbf{x}^{\delta_3} \xrightarrow{4} \mathbf{x}$, namely:

$$\mathbf{x}^{\delta_1} = e^{\mathbf{A}_1 \delta_1 T} \mathbf{x}_0 + \int_0^{\delta_1 T} e^{\mathbf{A}_1 \mu} \mathbf{b}_2 d\mu + \int_0^{\delta_1 T} e^{\mathbf{A}_1 \mu} \mathbf{b}_1 d\mu$$
$$\mathbf{x}^{\delta_2} = e^{\mathbf{A}_2 d_2 T} \mathbf{x}^{\delta_1} + \int_{\delta_1 T}^{\delta_2 T} e^{\mathbf{A}_2 \mu} \mathbf{b}_2 d\mu + \int_{\delta_1 T}^{\delta_2 T} e^{\mathbf{A}_2 \mu} \mathbf{b}_1 d\mu$$
$$\mathbf{x}^{\delta_3} = e^{\mathbf{A}_3 d_3 T} \mathbf{x}^{\delta_2} + \int_{\delta_2 T}^{\delta_3 T} e^{\mathbf{A}_3 \mu} \mathbf{b}_2 d\mu + \int_{\delta_2 T}^{\delta_3 T} e^{\mathbf{A}_3 \mu} \mathbf{b}_1 d\mu$$
$$\mathbf{x} = e^{\mathbf{A}_4 (1-\delta_3) T} \mathbf{x}^{\delta_3} + \int_{\delta_3 T}^{T} e^{\mathbf{A}_4 \mu} \mathbf{b}_2 d\mu + \int_{\delta_3 T}^{T} e^{\mathbf{A}_4 \mu} \mathbf{b}_1 d\mu$$

where $d_2 = \delta_2 - \delta_1$ and $d_3 = \delta_3 - \delta_2$. System (4) is equivalent to

$$\dot{\mathbf{x}} = \begin{bmatrix} \frac{di_{ca}}{dt} \\ \frac{di_{cb}}{dt} \\ \frac{V_{dc}}{dt} \end{bmatrix} = \mathbf{F}(\delta) \begin{bmatrix} i_{ca} \\ i_{ca} \\ i_{ca} \end{bmatrix} + \mathbf{g}(\delta) + \mathbf{h}(\omega, \delta) \tag{6}$$
$$\mathbf{y} = \mathbf{C}\mathbf{x}$$

Let

$$\boldsymbol{\varphi}_1^{\delta_1} = e^{\mathbf{A}_1 \delta_1 T}, \boldsymbol{\gamma}_1^{\delta_1} = \int_0^{\delta_1 T} e^{\mathbf{A}_1 \mu} \mathbf{b}_2 d\mu, \boldsymbol{\theta}_1^{\delta_1} = \int_0^{\delta_1 T} e^{\mathbf{A}_1 \mu} \mathbf{b}_1 \omega d\mu$$
$$\boldsymbol{\varphi}_1^{\delta_2} = e^{\mathbf{A}_2 \delta_2 T}, \boldsymbol{\gamma}_1^{\delta_2} = \int_{\delta_1 T}^{\delta_2 T} e^{\mathbf{A}_2 \mu} \mathbf{b}_2 d\mu, \boldsymbol{\theta}_1^{\delta_1} = \int_{\delta_1 T}^{\delta_2 T} e^{\mathbf{A}_2 \mu} \mathbf{b}_1 \omega d\mu$$
$$\boldsymbol{\varphi}_1^{\delta_3} = e^{\mathbf{A}_3 \delta_3 T}, \boldsymbol{\gamma}_1^{\delta_3} = \int_{\delta_2 T}^{\delta_3 T} e^{\mathbf{A}_3 \mu} \mathbf{b}_2 d\mu, \boldsymbol{\theta}_1^{\delta_3} = \int_{\delta_2 T}^{\delta_3 T} e^{\mathbf{A}_3 \mu} \mathbf{b}_1 \omega d\mu$$
$$\boldsymbol{\varphi}_0^{1-\delta_3} = e^{\mathbf{A}_4 \delta_1 T}, \boldsymbol{\gamma}_0^{1-\delta_3} = \int_{\delta_3 T}^{T} e^{\mathbf{A}_4 \mu} \mathbf{b}_2 d\mu, \boldsymbol{\theta}_0^{1-\delta_3} = \int_{\delta_3 T}^{T} e^{\mathbf{A}_4 \mu} \mathbf{b}_1 \omega d\mu$$

So

$$\mathbf{F}(\delta) = \boldsymbol{\varphi}_0^{1-\delta_3} \boldsymbol{\varphi}_1^{\delta_3} \boldsymbol{\varphi}_1^{\delta_2} \boldsymbol{\varphi}_1^{\delta_1}$$
$$\mathbf{g}(\delta) = \boldsymbol{\varphi}_0^{1-\delta_3} \boldsymbol{\varphi}_1^{\delta_3} \boldsymbol{\varphi}_1^{\delta_2} \boldsymbol{\gamma}_1^{\delta_1} + \boldsymbol{\varphi}_0^{1-\delta_3} \boldsymbol{\varphi}_1^{\delta_3} \boldsymbol{\gamma}_1^{\delta_2} + \boldsymbol{\varphi}_0^{1-\delta_3} \boldsymbol{\gamma}_1^{\delta_3} + \boldsymbol{\gamma}_0^{1-\delta_3}$$

IV. LINEARIZED SYSTEMS

$\mathbf{F}(\delta)$ and $\mathbf{g}(\delta)$ are nonlinear functions for the input. Therefore, we need to linearize the system. First, we define the following:

Definition 1: If the system three-phase compensating current is zero, the APF output voltage is $v_{cj} = v_{sj} - r_{sj} i_{sj}, (j = a, b, c)$. In one cycle of modulation, the output voltage v_{cj} that corresponds to the PWM function is δ(t) = [δ1(t), δ2(t), δ3(t)] $\delta(t) = [\delta_1(t), \ \ \delta_2(t), \ \ \delta_3(t)]$. If all this occurs, then we say the three-phase APF is in equilibrium:

$$\psi_{\delta,x} = \{(\delta(t), x_0(t)) | q(\delta(t), x_0(t)) = 0, \quad t \in R\}$$

If a system is in equilibrium, the neighborhood of state difference will be defined as $\Delta\mathbf{x} = \mathbf{x} - \mathbf{x_0}$, and the input difference will be defined as $\Delta\delta = \delta - \delta(t)$. Then, system (6) in the neighborhood of the state difference can be linearized as [8]

$$\begin{aligned}\Delta\dot{\mathbf{x}} &= \mathbf{F}(\delta(t))\Delta\mathbf{x}+\bar{\mathbf{G}}(\delta(t))\Delta\delta+\mathbf{H}(\boldsymbol{\omega})\boldsymbol{\omega}\\ \Delta\mathbf{y} &= \mathbf{C}\Delta\mathbf{x}\end{aligned} \tag{7}$$

where in

$$\bar{\mathbf{G}}(\delta(t))=\left[\bar{G}_1(\delta(t)) \quad \bar{G}_2(\delta(t)) \quad \bar{G}_3(\delta(t))\right]$$

$$=\begin{bmatrix} \left.\frac{\partial F(\delta)}{\partial\delta_1}\right|_{\delta_1} x_0+\left.\frac{\partial g(\delta)}{\partial\delta_1}\right|_{\delta_1}+\left.\frac{\partial h(\delta,\omega)}{\partial\delta_1}\right|_{\delta_1} \\ \left.\frac{\partial F(\delta)}{\partial\delta 2}\right|_{\delta_2} x_0+\left.\frac{\partial g(\delta)}{\partial\delta_2}\right|_{\delta_2}+\left.\frac{\partial h(\delta,\omega)}{\partial\delta_2}\right|_{\delta_2} \\ \left.\frac{\partial F(\delta)}{\partial\delta_3}\right|_{\delta_3} x_0+\left.\frac{\partial g(\delta)}{\partial\delta_3}\right|_{\delta_3}+\left.\frac{\partial h(\delta,\omega)}{\partial\delta_3}\right|_{\delta_3} \end{bmatrix}$$

$$H(\omega)=\left[H(\boldsymbol{\omega}) \quad H(\boldsymbol{\omega}) \quad H(\boldsymbol{\omega})\right]$$

$$=\begin{bmatrix} \left.\frac{\partial h(\boldsymbol{\omega},\delta)}{\partial\omega_{la}}\right|_{\omega} & \left.\frac{\partial h(\boldsymbol{\omega},\delta)}{\partial\omega_{lb}}\right|_{\omega} & 0 \end{bmatrix}$$

V. Optimal Design

Fig. 5 shows the optimized controller design logic diagram.

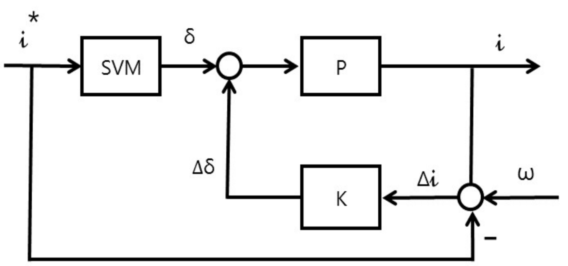

Fig. 5. The optimized controller design logic diagram.

We can achieve the output signal modulation by tracking the output signal and the interference signal feedback to the controller. Fig. 5 can be simplified as Fig. 6. We design a feedback controller that makes the closed-loop system (7) asymptotically stable, and the closed-loop transfer function $\mathbf{T}_{\boldsymbol{\omega}\mathbf{z}}$ satisfies

$$\|\mathbf{T}_{\boldsymbol{\omega}\mathbf{z}}\|_\infty=\sup_{\boldsymbol{\omega}\neq 0}\frac{\|\mathbf{z}\|_2}{\|\boldsymbol{\omega}\|_2}<1$$

A state control law having such properties is called an H∞ control law of the system (7).

Theorem 1: In system (7), there exists a state feedback H∞ controller if and only if there exists a symmetric positive definite matrix X and a matrix W, such that the following matrix inequality (8) holds: [9] [10]

$$\begin{bmatrix} F(\delta(t))X+G(\delta(t))W+(F(\delta(t))X+G(\delta(t))W)^T & H(\omega) & X^T \\ G(\delta(t))^T & -I & 0 \\ X & 0 & -I \end{bmatrix}<0 \tag{8}$$

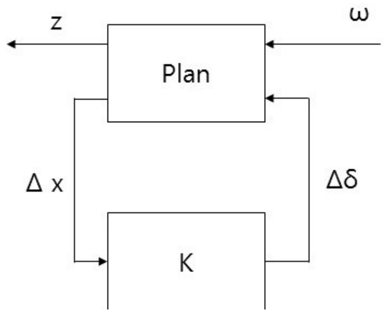

Fig. 6. Standard form.

Furthermore, if for inequality (8) there is a feasible solution X^*, W^*, then

$$\Delta\delta = WX^{-1}\Delta\mathbf{x}=K\Delta\mathbf{x}$$

is system (7) in a state feedback H_∞ controller.

For a given scalar $\gamma>0$, to obtain a γ-suboptimal controller with state feedback H_∞, we consider the condition of a transfer function as

$$\|T_{\omega z}\|_\infty<\gamma \Leftrightarrow \gamma^{-1}\|T_{\omega z}\|_\infty<0$$

In this case, the corresponding matrix inequalities (8) become

$$\begin{bmatrix} F(\delta(t))X+G(\delta(t))W+(F(\delta(t))X+G(\delta(t))W)^T & H(\omega) & X^T \\ G(\delta(t))^T & -I & 0 \\ X & 0 & -\gamma^2 I \end{bmatrix}<0 \tag{9}$$

By using the applicable LMI Toolbox feasp solver, the matrix inequality can be solved.

Further, based on the γ-suboptimal controller for state feedback H_∞, an optimization problem can be obtained:

$$\begin{aligned}&\min \rho\\ &\text{s.t.}\\ &\begin{bmatrix} F(\delta(t))X+G(\delta(t))W+(F(\delta(t))X+G(\delta(t))W)^T & H(\omega) & X^T \\ G(\delta(t))^T & -I & 0 \\ X & 0 & -\rho I \end{bmatrix}<0\\ &X>0\end{aligned} \tag{10}$$

If the solution exists, the system can obtain an H_∞ optimal controller.

Problem (10) can be solved by applying the LMI Toolbox mincx.

VI. Conclusion

Power electronic circuits comprise discrete event dynamic systems and continuous variable dynamic systems. To improve performance, a model power electronic circuit using a switching system is necessary and feasible.

This paper uses a linear approximation. The system does not reach 100% accuracy. Thus, part of the linear approximation should be improved.

This research paper models the equivalent of an APF. Other power electronic circuits provide reference values for further study

ACKNOWLEDGMENT

The authors would like to acknowledge that their research has been co-financed by Korea Electric Power Corporation through the Korea Electrical Engineering & Science Research Institute.

REFERENCES

[1] D. Liberzon, *Switching in Systems and Control*, Birkhauser Boston, 2003, ch.1.

[2] Q. Li *et al*., "Modeling and stability analysis of three-phase converter based on switching system theory," *Transactions of China Electro Technical Society*, vol. 24, no. 11, Nov. 2009.

[3] G. J. Lee, M. M. Albu, and G. T. Heydt, "A power quality index based on equipment sensitivity," *IEEE Trans. on Power Delivery*, vol. 19, no. 3, pp.1054–1510, Jul. 2004.

[4] H. Akagi, "New trends in active filters for power conditioning," *IEEE Trans. on Industry Applications*, vol. 32, no. 6, pp. 1312–1322, Nov. 1996.

[5] H. Akagi *et al*., "A shunt active filter based on voltage detection for harmonic termination of radial power distribution line," *IEEE Trans. on Industry Applications,* vol. 35, no. 3, pp. 638–645, May/Jun. 1999.

[6] N. Mohan, T. M. Undeland, and W. P. Robbins, *Power Electronics Converters, Applications and Design*, Wilkey & Sons, 2003, ch. 8.

[7] A. M. Hava, R. J. Kerkman, and T. A. Lipo, "Simple analytical and graphical methods for carrier-based PWM-VSI divers," *IEEE Trans. on Power Electronics*, vol. 14, no. 1, pp. 49–61, Jan. 1999.

[8] K. Hassan, *Nonlinear Systems*, 3rd ed., Marcia Horton, Prentice Hall, 2002, ch.12, ch.13

[9] C. Olalla, R. Leyva, A. E. Aroudi, and I. Queinnec, "Robust LQR control for PWM converters: an LMI approach," *IEEE Trans. on Industrial Electronics*, vol. 56, no. 7, pp. 2548–2558, July 2009.

[10] Li Yu, *Robust Control-The Processing of the Linear Matrix Inequality (lmi) Approach*, 1st ed. Y.-B. Zhu, C.N.: Tsinghua University Press, 2002, ch.3, ch.4.

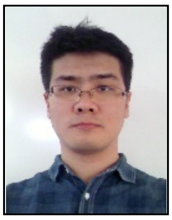

Hui Song was born in 1990, China. He received the B.S. degree in Electrical Engineering from Chungnam National University, Daejeon, Korea, in 2015. He is currently the M.S. course at Chungnam National University. His research interests include switched system and power system.

Eun-Sung Gil was born on January 11, 1990, Daejeon, Korea. He received the B.S. degree in Electrical Engineering from Chungnam National University, Daejeon, Korea, in 2015. He is currently the M.S. course at Chungnam National University. His research interests include power system, HVDC system, and automatic control

Kwan-Ho Chun was born in 1970, Korea. He received the B.S., M.S. and the Ph.D. degrees in Electrical Engineering from Seoul National University, in 1993, 1995 and 2002, respectively. From 2002 to 2004, he worked for SAMSUNG Electronics Co., KOREA as a senior Engineer. From 2004 to 2013, he was a senior engineer of TOSHIBA SAMSUNG Storage Technology Co., KOREA. Since 2013, he has been with the Department of Electrical Engineering at Chungnam National University, Daejeon, Korea, where he is currently an Associate Professor. His research interests include nonlinear systems theory, switched system control theory and applications in robotics, renewable energy and electrical power systems.

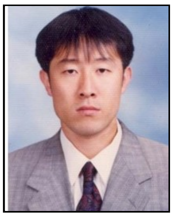

Sang-Ho Park obtained the B.S. and M.S. degree in Electrical Engineering from Myongji,Seoul, Korea,in 2000 and 2002, respectively. Currently he is a Senior Researcher in the Power system lab at the KEPCO Research Institute. His research interests include power quality and Offshore Windpower generations.